

Line-of-Sight Anisotropies within X-ray Luminous Cluster Samples

Christopher J. Miller¹, Michael J. Ledlow², David J. Batuski¹

¹*Department of Physics and Astronomy, University of Maine, Orono, Maine 04469-5709, U.S.A.*

²*Institute for Astrophysics, University of New Mexico, Albuquerque, New Mexico 87131, U.S.A.*

26 April 2024

ABSTRACT

We present the results from two-point spatial correlation analyses on X-ray confirmed northern Abell clusters. The cluster samples are subsets of a volume-limited ROSAT All-Sky Survey study of 294 $R \geq 0$ Abell clusters of which 240 are X-ray luminous. This large number of clusters has allowed for magnitude- and volume-complete samples to be analysed according to richness and X-ray luminosity. For $R \geq 1$ clusters, we find $r_0 = 22h^{-1}\text{Mpc}$ and $\gamma = -1.7$, which is consistent with previous analyses of visually selected $R \geq 1$ Abell clusters. We also find no indications of line-of-sight anisotropies within the $R \geq 1$ clusters. For $R \geq 0$ clusters, we find $r_0 = 17.5h^{-1}\text{Mpc}$ (and $\gamma = -1.8$) which is considerably lower than recent determinations of the correlation length for similar $R \geq 0$ X-ray bright cluster samples (e.g. the X-ray Brightest Abell Cluster sample (XBACs) with $21 \leq r_0 \leq 26h^{-1}\text{Mpc}$ and the RASS1 X-ray cluster sample with $r_0 \sim 23h^{-1}\text{Mpc}$). All of the $R \geq 0$ X-ray confirmed samples, including the XBACs and RASS1 clusters show line-of-sight anisotropies. Since X-ray emissions confirm a cluster's reality, we conclude that these line-of-sight anisotropies are not the result of spuriously selected clusters. These results conflict with past conclusions that the correlation length of $R \geq 0$ Abell clusters is artificially enhanced due to anisotropies caused by spurious cluster selection. We also examine a magnitude- and volume-complete sample of $R \geq 1$ Abell clusters for the dependence of r_0 and γ on X-ray luminosity, and find no evidence for r_0 to grow with increasing X-ray luminosity thresholds. This is contrary to similar L_x vs. r_0 analyses of the RASS1 and XBACs cluster samples. We describe selection effects within

the flux-limited XBACs and RASS1 samples and suggest how they can affect both the size of the correlation length and its dependence on L_x .

Key words: cosmology: theory - galaxies:clusters - large-scale structure of Universe - X-rays:galaxies

1 INTRODUCTION

The two-point spatial correlation function is used to describe the scale of clustering within discrete datasets. Both galaxies and clusters of galaxies have a functional power-law form for the correlation function, $\xi(r) = (r/r_0)^\gamma$. The slope and amplitude of this power law is rather well-defined for galaxies to be $r_0 = 5h^{-1}\text{Mpc}$ and $\gamma = -1.8$ (*e.g.* Willmer et al. 1998 and references therein). For galaxy clusters, the slope has been established at $-2.0 \leq \gamma \leq -1.8$, but the value for r_0 has been a matter of much debate. The majority of cluster-cluster spatial correlation analyses have been based on the visually “scanned” Abell and ACO catalogs (Abell 1958; Abell, Corwin and Olowin 1989) and the machine scanned Automatic Plate Measuring (APM) Facility Cluster Survey (Maddox et al. 1990a,b). The correlation length for the visually selected clusters is $\sim 20 - 25h^{-1}\text{Mpc}$ with positive correlations out to separations of $\sim 50h^{-1}\text{Mpc}$ (*e.g.* Miller et al. 1999 and references therein). However, the clusters selected through machine scanning have $r_0 \sim 15h^{-1}\text{Mpc}$ and little positive correlation beyond 25^{-1}Mpc (Efstathiou et al. 1992; Dalton et al. 1994).

The large differences between the above determinations of r_0 for clusters have been explained in either of two ways:

(i) The optically selected clusters suffer from spurious cluster selection. This observational selection bias occurs when two clusters are near each other on the plane of the sky, but separated by a large distance radially. When this occurs, the richness of either the foreground or background cluster may be artificially enhanced due to projection effects. This line-of-sight selection bias creates false spatial correlations at larger separations, which in turn inflates r_0 (e.g. Sutherland 1988; Efstathiou et al. 1992). We point out that a substantial number of clusters missed in a non-random systematic manner during the visual selection process can also give rise to this effect.

(ii) The value of r_0 is dependent on the mean cluster number density (n_c) of the sample, $r_0 = 0.4n_c^{-1/3}$. (1)

In this case, the APM clusters should have a smaller correlation length since their number

density is nearly four times that of $R \geq 1$ Abell clusters (Bahcall & West 1992; Bahcall & Cen 1994).

While both of the above solutions seem plausible and explain (and/or correct) the value of r_0 , both solutions have also been shown to be flawed. Line-of-sight anisotropies within the Abell and ACO catalogs have been examined in detail by Miller et al. (1999) who find that only $\sim 10\%$ of clusters in the ENACS (Katgert et al. 1996) and MX (Slingsend et al. 1998) surveys show strong background/foreground contaminations. In addition, Miller et al. find $r_0 \sim 22h^{-1}\text{Mpc}$ for $R \geq 1$ clusters both before and after removing these contaminated clusters from the analysis. They also show that the minimal anisotropy present in the $R \geq 1$ subset of clusters is similar in scale to that of the APM clusters. Miller et al. conclude that projection effects and line-of-sight anisotropy are not large problems for $R \geq 1$ Abell/ACO clusters and do not artificially enhance r_0 .

On the other hand, the density dependence on the correlation length was determined empirically and ultimately depends on the accurate evaluation of r_0 and the mean cluster density for multiple samples. While many of the currently available cluster datasets have mean densities $\sim 1 \times 10^{-5}h^3\text{Mpc}^{-3}$ or greater, until recently, only the richest ($R \geq 1$) Abell clusters have provided r_0 for datasets with densities $\sim \times 10^{-6}h^3\text{Mpc}^{-3}$. Croft et al. (1997) constructed a catalog of very rich APM clusters with a mean number density of $\sim 1 \times 10^{-6}h^3\text{Mpc}^{-3}$ and find $r_0 = 21h^{-1}\text{Mpc}$ which is contrary to the expected result from Equation (1). Unfortunately, we do not have a statistically significant determination of r_0 for $R \geq 2$ Abell clusters (with $\bar{n} \sim 1 \times 10^{-6}h^3\text{Mpc}^{-3}$), although results from Peacock & West (1992) suggest that the correlation length may be as high as $r_0 = 45h^{-1}\text{Mpc}$. With only two very rich samples studied so far, the $r_0 \propto n_c^{-1/3}$ relation lacks strong observational support for densities less than $10^{-5}h^3\text{Mpc}^{-3}$. In addition to the observational analyses, both Croft & Efstathiou (1994) and Eke et al. (1996) find that the density dependence on the correlation length is at best very weak in N-body simulations.

In this work, we will examine magnitude-limited and volume-limited samples of Abell clusters which are also X-ray luminous. The problems of projection effects and spurious cluster selection are minimized in X-ray bright clusters, allowing a more reliable determination of the amplitude and slope of the two-point spatial correlation function. We would expect that any line-of-sight anisotropies present in optically limited samples would not be present in X-ray confirmed cluster samples. However, while the X-ray emission of the intracluster

gas will confirm the reality of a catalogued cluster, this approach provides no information on clusters missed by Abell (1958) in his visual search. With the recent work on X-ray selected cluster catalogs (e.g. Ebeling et al. 1998; Vikhlinin et al. 1998), we can expect future two-point spatial correlation analyses that would include any optically missed galaxy clusters as well (see De Grandi et al. 1999).

2 DATA AND METHODS

The X-ray luminosities and their associated uncertainties were taken from Voges, Ledlow, Owen and Burns (1999). Voges et al. studied RASS (ROSAT All-Sky Survey) data for a volume limited ($z \leq 0.09$) sample of 294 $R \geq 0$ Abell clusters. These clusters have the following criteria: $\log_{10} N_H < 20.73$ (roughly corresponding to $|b| \geq 25^\circ$ which we apply as a cut-off), $z \leq 0.09$ and $\delta \geq -27^\circ$. All of the X-ray luminous Abell clusters used in this work have measured redshifts. Voges et al. found that 84% of the $R \geq 0$ Abell clusters in their volume-limited sample were X-ray luminous. The majority of the clusters that showed no X-ray emissions were $R = 0$ clusters.

We apply magnitude and richness constraints to the Voges et al. sample so that we may examine statistically complete samples. Specifically, we will divide the clusters into two subsets with different richness class ranges, one with $R \geq 0$ and the other with $R \geq 1$. For each of these richness-limited subsets, we will look at volume-limited ($z \leq 0.09$) cluster samples with and without appropriate magnitude limits so that they may be considered statistically complete for comparison to other such analyses. For the $R \geq 0$ clusters, we will use a magnitude limit of $m_{10} \leq 16.5$ and for $R \geq 1$ clusters we will use $m_{10} \leq 16.8$. Postman, Huchra, & Geller (1992-hereafter PHG) presented correlation analyses for the magnitude-complete sample of $R \geq 0$, $m_{10} \leq 16.5$ clusters. Miller et al. (1999) presented correlation analyses for the magnitude-complete sample of $R \geq 1$, $m_{10} \leq 16.8$ clusters. Both of these samples were based on visually selected clusters.

The dependence of the X-ray luminosity on cluster mass ($L_x \propto M^p$) has been well established both analytically and numerically (Bertschinger 1985; Evrard & Henry 1991; Navarro, Frenk, and White 1995, Ledlow et al. 1999). Figure 1 shows the observational results of the $L_x - M$ relation using 42 cluster virial-masses from Girardi et al. (1998). An outlier-resistant linear-fit to the data in Figure 1 produces $L_x \propto M^{2.38 \pm 1.27}$. The errors bars on each data point are 1σ Poisson in the virial mass determination as provided by Girardi et

al. and 1σ in the X-ray luminosity determination from Voges et al. This observational result for p is consistent with simulations by Ledlow et al., but is significantly steeper than the self-similar scaling laws of Kaiser (1986) which predicts $L_x \propto M^{4/3}$. The analytical, numerical, and observational evidence for $L_x \propto M^p$ suggests that we should also examine the cluster-cluster correlation function for dependence on X-ray luminosity. Such a dependence has been found in the XBACs and the RASS1 clusters, although both results can not be considered statistically significant (Abadi et al. 1998; Borgani et al. 1999; Moscardini et al. 1999).

We use the following estimator derived in Hamilton (1993) for the determination of the correlation function:

$$\xi(r) = \frac{DD(r) \times RR(r)}{DR(r)^2} - 1, \quad (2)$$

where DD , RR , and DR are the data-data, random-random and data-random paircounts respectively with separations between $r - \frac{\Delta r}{2}$ and $r + \frac{\Delta r}{2}$. We refer the reader to Hamilton (1993) and Landy & Szalay (1993) for an analytical analysis of the estimator. Compared to previous estimators (Bahcall & Soneira 1983; PHG), this one is proposed to be less affected by uncertainties in the mean number density where separations are large and ξ is small. Recently, Ratcliffe et al. (1998) used N-body simulations to show that Equation (2) provided the most accurate results when compared to other estimators.

The random paircounts (DR , RR) are evaluated by averaging over 400 catalogs generated with the same number of pseudo-clusters as the sample under consideration. The angular coordinates in these catalogs are randomly assigned with the same boundary conditions as the survey. While cluster X-ray emission is not entirely hidden due to galactic obscuration, the clusters themselves were catalogued optically (note: corrections to the X-ray luminosities were made by Voges et al. (1999) to account for galactic absorption), therefore, the known selection bias in b is carried into all subsets of the original catalog. To account for this, we apply a latitude selection function;

$$P(b) = 10^{\alpha(1 - \csc|b|)}, \quad (3)$$

with $\alpha = 0.32$. The redshifts assigned to the random catalog points are selected from the observed data after being smoothed with a Gaussian of width 3000 km s^{-1} . This technique corrects for radial density gradients on small scales in the observed distribution. Distances to all clusters were calculated assuming a Friedman universe with $q_0 = 0$ and $H_0 = 100 \text{ km s}^{-1} \text{ Mpc}^{-1}$.

Table 1. Results for the Power-Law Fits of ξ

Sample	Size	R	m_{10}	γ	r_0 ($h^{-1}\text{Mpc}$)
1	189	≥ 0	≤ 16.5	-1.78 ± 0.20	$17.7^{+3.8}_{-4.5}$
2	240	≥ 0	all	-1.87 ± 0.18	$17.3^{+3.0}_{-2.7}$
3	117	≥ 1	≤ 16.8	-1.70 ± 0.25	$21.5^{+6.2}_{-7.0}$
4	130	≥ 1	all	-1.68 ± 0.22	$22.4^{+5.9}_{-6.8}$

3 RESULTS

The results for power law fits to the cluster-cluster two-point spatial correlation function are given in Table 1 and Figures 2 and 3. It is important to note that samples 2 and 4 are volume-limited only and are incomplete in magnitude. Volume-limited surveys are not well suited for comparison to other works, since some very dim but nearby clusters will be added to the volume over time. For instance, since the time the Voges et al. volume-limited optically complete sample was defined, an additional 86 clusters have since been observed that are within $z = 0.09$. This is nearly a 30% increase in only a few years time. On the other hand, a magnitude-limited sample will always contain the same number of clusters (if complete). The error bars in Figure 2 are determined from

$$\delta\xi = \frac{(1 + \xi)}{\sqrt{DD}}. \quad (4)$$

However, we note that Croft & Efstathiou (1994) have shown that this underestimates the true error by a factor of $1.3 \rightarrow 1.7$.

There are significant differences in r_0 and γ between the $R \geq 0$ clusters and the $R \geq 1$ clusters. The two most important aspects of these results are:

(i) γ and r_0 for sample 1 differ significantly from those of PHG who find $r_0 = 20.0h^{-1}\text{Mpc}$ and $\gamma = -2.5$ for an optically selected ($m_{10} \leq 16.5$, $z \leq 0.08$) complete sample of $R \geq 0$ clusters. If we constrain the slope for sample 1 to that of PHG, we find $r_0 = 13.5h^{-1}\text{Mpc}$ which differs from their results by 2σ .

(ii) The results for samples 3 and 4 confirm a large correlation length for $R \geq 1$ clusters as seen previously by Bahcall & Soneira (1983), PHG, Peacock & West (1992) and Miller et al. (1999), using visually selected Abell clusters.

We can compare the results for r_0 to those predicted by the average number densities, \bar{n} , for samples 1 and 3. PHG report $\bar{n} = 1.2 \times 10^{-5}h^3\text{Mpc}^{-3}$ for $R \geq 0$ Abell clusters (*i.e.* sample 1), while Miller et al. (1999) report $\bar{n} = 6.6 \times 10^{-6}h^3\text{Mpc}^{-3}$ for $R \geq 1$ Abell clusters. Using these densities, Equation (1) predicts $r_0 = 17.5h^{-1}\text{Mpc}$ and $r_0 = 21.3h^{-1}\text{Mpc}$ for

Table 2. Results from Other X-ray $R \geq 0$ Cluster Surveys

Reference	Cluster Sample	$N_{clusters}$	$r_0(h^{-1}Mpc)$	γ
Nichol <i>et al.</i> 1994	Abell	67	16.1 ± 3.4	-1.9 ± 3.4
Abadi <i>et al.</i> 1998	XBACs	248	$21.1^{+1.6}_{-2.3}$	-1.92
Moscardini <i>et al.</i> 1999	RASS1	130	22.7 ± 3.6	$-2.08^{+0.43}_{-0.51}$
Borgani <i>et al.</i> 1999	XBACs	203	26.0 ± 4.5	-2.00 ± 0.4
This work	Abell	240	$17.3^{+3.0}_{-2.7}$	-1.87 ± 0.18

Table 3. Correlation function as a function of increased luminosity cut-off.

Sample	Size	$L_x \times 10^{43}$ $h^{-2} \text{ergs s}^{-1}$	γ	r_0 ($h^{-1} \text{Mpc}$)	r_0 for $\gamma = -1.8$ ($h^{-1} \text{Mpc}$)
5	103	≥ 0.14	-1.88 ± 0.32	$22.2^{+10.5}_{-11.1}$	23.1
6	93	≥ 0.28	-1.99 ± 0.45	$17.4^{+11.2}_{-12.4}$	19.2
7	80	≥ 0.42	-2.30 ± 0.49	$17.2^{+11.6}_{-13.0}$	20.8
8	71	≥ 0.56	-2.52 ± 0.60	$15.0^{+13.0}_{-13.4}$	19.0

samples 1 and 3 respectively. If there are a substantial number of spuriously selected $R = 0$ clusters in the PHG sample, their calculated number density would be over-estimated. Using the methods of Miller *et al.* (1999), we calculate $\bar{n} = 8.68 \times 10^{-6} h^3 \text{Mpc}^{-3}$ using only X-ray luminous Abell clusters (i.e. Sample 2), which corresponds to $r_0 = 19.5 h^{-1} \text{Mpc}$. These predictions are well within the 1σ uncertainties on r_0 given in Table 1. In Table 2, we list other two-point correlation function results for X-ray bright cluster samples that include $R \geq 0$ clusters. Our results are most similar to those of Nichol *et al.* (1994). We discuss possible explanations for the differences in the values of r_0 in Section 3.2.

3.1 Anisotropies within X-ray Cluster Samples

At this point, we should also examine these samples for line-of-sight anisotropies such as those found in the PHG $R \geq 0$ sample (Efstathiou *et al.* 1992). Line-of-sight anisotropies have been suggested by many to be responsible for the high value of r_0 found by PHG in the $R \geq 0$ clusters. The only other work on anisotropies in X-ray confirmed cluster samples was performed by Nichol *et al.* (1994). Their sample of 67 $R \geq 0$ Abell clusters has little line-of-sight anisotropy and a correlation length of $r_0 = 16 h^{-1} \text{Mpc}$ which is significantly lower than that found by PHG (note: both the Nichol and PHG samples are $R \geq 0$). Sutherland (1988) was the first to show that by dividing the pair separation vector (\vec{r}) into its line-of-sight (π) and perpendicular-to-the-line-of-sight (σ) components, one can look for strong correlations in $\xi(\sigma, \pi)$ where σ is small ($0 - 20 h^{-1} \text{Mpc}$) and π is large ($30 - 100 h^{-1} \text{Mpc}$). Sutherland

suggested that if such line-of-sight anisotropies exist, there must be a substantial amount of spurious cluster selection due to foreground/background contamination. Clearly, if the clusters are confirmed by their X-ray brightness (which is not affected by projection effects), then we would expect no spurious clusters and little line-of-sight anisotropy (as seen in the Nichol et al. results).

In Figures 4 and 5 we present contour plots of $\xi(\sigma, \pi)$ for samples 1 and 3. The bold line is $\xi(\sigma, \pi) = 1$, indicative of relatively strong correlations. In an ideal sample with no line-of-sight anisotropies, small cluster peculiar velocities and non-elongated superclusters, one might hope to find $\xi > 1$ contours with similar extent (say $25h^{-1}\text{Mpc}$) in σ and π . Notice that the $R \geq 0$ clusters show strong correlations for $\sigma < 20h^{-1}\text{Mpc}$ and π out to $80h^{-1}\text{Mpc}$. This indicates that an unexpectedly large number of clusters pairs have small separations on the plane of the sky, while being separated by large distances radially. Our $R \geq 0$ subset shows the same strong anisotropies seen in the optical sample of $R \geq 0$ clusters presented by Efstathiou et al. (1992), even though all clusters have been confirmed by their X-ray emission. Therefore, while some type of anisotropy does exist in the $R \geq 0$ subset, it is not the result of spuriously selected clusters.

Both of the samples that exclude $R = 0$ clusters show no indications of line-of-sight anisotropies in Figure 5. This supports claims made by Miller et al. (1999) that the $R \geq 1$ subset of Abell clusters do not suffer from serious projection contamination and line-of-sight anisotropies. In addition, the value of r_0 for X-ray selected $R \geq 1$ Abell clusters is similar to that found by Miller et al. using their newly enlarged sample of Abell/ACO clusters with measured redshifts. It is important to recognize that the subsets showing the most line-of-sight anisotropies have the lowest value for r_0 . This is precisely the opposite of what has been suggested by Sutherland (1992), Efstathiou et al. (1992), Dalton et al. (1994) and Nichol et al. (1994) among others (see section 1). From these results we conclude that the correlation length is affected by the richness of the cluster sample and that Equation 1 works well for the samples analysed here, although we point out that a higher richness class sample (i.e. $R \geq 2$) is needed to verify such a relation for all richness classes. We conclude that while line-of-sight anisotropies are present in the $R \geq 0$ samples, there is no indication that they artificially inflate the correlation length.

3.2 Comparison to Other X-ray Samples

With the recent increases in the amount of available X-ray data for clusters, other X-ray cluster samples have also been examined for structure using the two-point correlation function. Specifically, the Ebeling et al. (1996) XBACs sample is a flux-limited survey of Abell/ACO clusters in the northern and southern galactic hemispheres, and the De Grandi et al. (1999) RASS1 sample is a flux-limited survey of clusters in the Southern hemisphere. The two-point correlation function for the XBACs was presented by Abadi et al. as well as Borgani et al., while Moscardini et al. have presented correlation results for the RASS1 cluster samples. (The results for these studies are presented in Table 2).

The cluster sample in this work differs significantly from that of the XBACs sample which has a disproportionate distribution of richness classes. For instance, the XBACs sample contains 25% $R = 0$ clusters with an average redshift of $z \sim 0.073$, 39% $R = 1$ with an average redshift of $z = 0.085$, while the remaining $R \geq 2$ clusters have an average redshift of $z = 0.109$. For the Voges et al. $R \geq 0$ cluster Sample 1, 46% are $R = 0$ clusters with an average redshift of $z = 0.064$, 44% are $R \geq 1$ clusters with an average redshift of $z = 0.067$ and the remaining $R \geq 2$ clusters have an average redshift of $z = 0.066$. The XBACs sample is not homogenous in richness and includes nearby poorer clusters and generally more distant rich clusters. In Figure 6 we present the anisotropy plot for the XBACs sample. There is strong evidence for extreme line-of-sight anisotropy as the result of cluster pairs with small separations on the plane of the sky and large separations in redshift. It is of interest to note that a large fraction ($\sim 50\%$) of the cluster pairs causing this anisotropy are located within a very small range of R.A. ($0^h \leq \alpha \leq 3^h$) and 25% are located within an area of only ~ 0.04 steradians (corresponding to roughly 1% of the total area covered by the XBACs). While we cannot explain the apparent pair-selection bias in the XBACs sample, the disproportionate fraction of higher richness clusters in the XBACs is a direct result of flux-limited surveys (as shown by Bahcall & Cen 1994). Using the richness-dependence of the correlation length (Equation 1), a large fraction of $R = 1$ and $R \geq 2$ clusters would inflate the correlation length as compared to a sample containing a homogeneous distribution of richness class clusters ($R \geq 0$). [Note: a homogeneous richness distribution of Abell and ACO clusters is complicated by classification differences between the two catalogs (see e.g. David, Forman & Jones 1999).]

The RASS1 sample contains 130 clusters, the majority of which (101) are Abell/ACO

clusters. We examine the richness distribution of this sample and find that 11% are $R = 0$ clusters with an average redshift of $z = 0.066$, 22% are $R = 1$ clusters with an average redshift of $z = 0.094$ and 32% $R \geq 2$ clusters with an average redshift of $z = 0.104$. The remaining 29 clusters in the RASS1 sample are clusters “missed” by Abell/ACO. Most of these are poorer APM or Zwicky clusters while some are newly identified. The average redshift of these clusters is $z = 0.091$. In any event, the vast majority of clusters in this sample are Abell/ACO and many of the others would not have met Abell’s richness criteria. In Figure 7 we present the anisotropy plot for the RASS1 cluster sample. While the line-of-sight anisotropy is not as problematic as in the XBACs, there is still more than in the $R \geq 1$ Abell cluster sample examined in this work. As in the XBACs case, the large fraction of $R \geq 1$ clusters will increase the correlation length of the RASS1 sample (compared to the more homogeneously distributed Voges et al. sample).

3.3 L_x and Richness Dependence on r_0 and γ

From the $L_x - M$ relation shown in section 2, we are also interested in any trend in r_0 and γ with respect to L_x . We created four magnitude- and volume-limited samples with increasing L_x cutoffs. These samples are subsets of Sample 3 and the results for r_0 and γ are presented in Table 3. Notice that we see no increase in r_0 with respect to increased L_x . While at first glance it may appear as if r_0 is actually decreasing as we raise the L_x cutoff, this is simply the result of a steepening slope (the final column in Table 2 lists the value of r_0 when the slope is constrained to $\gamma = -1.8$). We also examined the other three samples and found no increase in r_0 with increasing L_x cutoff. These results contradict those using the XBACs and RASS1 clusters in which there is seen a weak dependence in r_0 with increasing L_x (Abadi, Lambas, & Muriel 1998; Borgani et al. 1999; Moscardini et al. 1999). However, none of the results based on the XBACs and RASS1 clusters can be considered statistically significant due to small sample sizes. Voges et al. have found a significant correlation between X-ray luminosity and cluster richness (where the probability of no correlation is $< 1 \times 10^{-4}$). Therefore, if a cluster sample has a disproportionate richness distribution (as in both the XBACs and the RASS1 clusters), r_0 will increase (due to the richness dependence on r_0) as the higher L_x cutoff excludes poorer clusters. Thus, the $r_0 - L_x$ dependence seen in the XBACs and RASS1 clusters is most likely an artefact of the biased cluster samples used in their analyses.

With the recent discovery by Loken, Melott, and Miller (1999) that X-ray cooling flow clusters with the highest mass deposition rates are located in dense cluster environments, we decided to examine the nearest-neighbor distribution (nnd) of the Voges et al. (1999) X-ray luminous Abell sample for any similar correlations. Specifically, we divided the sample into the same X-ray luminosity classes as described in Table 3 plus a class of clusters with no detected emissions. We then determined the average nearest-neighbor distance for each class. The clusters with no detected X-ray emissions had the smallest distance, $\langle nnd \rangle = 17.3h^{-1}\text{Mpc}$, with an increasing $\langle nnd \rangle$ for clusters with the highest X-ray luminosities ($L_x > 0.56 \times 10^{43}h^{-2}\text{ergs s}^{-1}$) with a distance of $\langle nnd \rangle = 19.6h^{-1}\text{Mpc}$. However, a K-S analysis of the nnd distributions show no significant differences among the luminosity classes examined. Thus, while a slight trend for the average nearest-neighbor distance to increase with increasing luminosity is detected, it is not of statistical significance.

4 CONCLUSIONS

We have analysed magnitude- and volume-limited samples of Abell clusters for the amplitude and slope of the two-point spatial correlation function and also for line-of-sight anisotropies. We find $r_0 = 17.5h^{-1}\text{Mpc}$ and $\gamma = -1.8$ for $R \geq 0$ clusters, which is consistent with the results of Nichol et al. (1994). However, we find that the $R \geq 0$ subset contains considerable line-of-sight anisotropies even after all clusters have been confirmed by their X-ray brightness. For $R \geq 1$ clusters we find $r_0 = 22h^{-1}\text{Mpc}$ and $\gamma = -1.7$ and no indications of line-of-sight anisotropy. We conclude that (1) some type of anisotropy is present in $R = 0$ clusters, although it is not the result of spuriously selected clusters. We suggest that this anisotropy could be caused by Abell systematically searching for (or noticing) $R = 0$ clusters only in the vicinity of richer clusters and therefore missing a substantial number of more isolated $R = 0$ clusters; (2) the correlation length is not artificially inflated by line-of-sight anisotropies; (3) there is a cluster richness dependence on r_0 (or mean density) in cluster subsets, although it is hard to say what effect the anisotropy in the $R = 0$ clusters has; (4) there is no correlation between r_0 and L_x for X-ray confirmed Abell clusters.

These results confirm the value for r_0 by previous studies using optically limited samples of $R \geq 1$ Abell clusters (Bahcall & Soneira 1983; Miller et al. 1999). Yet at the same time, we find no evidence for the correlation length to be artificially inflated as the result of spuriously selected cluster. Many researchers have advocated ‘corrective’ techniques for

dealing with $R \geq 0$ samples of Abell clusters. These techniques typically involve the exclusion of questionable clusters (or cluster pairs) from correlation analyses which, in turn, lowers r_0 considerably (Sutherland 1988; Efstathiou et al. 1992). Our findings indicate that, even after using X-ray confirmed $R = 0$ Abell clusters, as well as samples including clusters missed by Abell (the RASS1 sample), line-of-sight anisotropies are still present. The only X-ray cluster sample that shows no such anisotropy is the $R \geq 1$ Abell cluster subset. We find little difference in r_0 between visually selected clusters ($r_0 \sim 22h^{-1}\text{Mpc}$, Miller et al. 1999) and X-ray confirmed $R \geq 1$ Abell clusters ($r_0 = 22h^{-1}\text{Mpc}$, presented in this work) for similar slopes ($-1.8 \leq \gamma \leq -1.7$).

The correlation length for rich clusters of galaxies has been debated for well over a decade. During that time, no other cluster catalog has been examined in such great detail as the Abell catalog. The discovery of line-of-sight anisotropies present in $R = 0$ clusters is a direct result of the catalog's detailed analysis (Sutherland 1988; Efstathiou 1992; Peacock & West 1992). These anisotropies in the $R = 0$ clusters have led many researchers to conclude that the correlation length of Abell clusters is artificially enhanced and is not an accurate estimation of the scale of clustering in the local Universe. A large correlation length with clustering on scales $\sim 50h^{-1}\text{Mpc}$ is not consistent with standard CDM models. These results provide continuing evidence for a large correlation length for rich clusters, which must be represented in cosmological evolutionary scenarios.

Acknowledgments

CM was funded in part by the National Aeronautics and Space Administration and the Maine Science and Technology Foundation. M.J.L was supported in part by NASA grant NAG5-6739.

REFERENCES

- Abadi, M., Lambas, D., and Muriel, H. 1998, *ApJ*, 507, 526
- Abell, G. O. 1958, *ApJS*, 3, 211
- Abell, G. O., Corwin, H. G., Olowin, R. P. 1989, *ApJS*, 70, 1 (ACO)
- Bahcall, N.A. & Cen, R. 1994, *ApJL*, 426, L15
- Bahcall, N., Soniera, R. 1983, *ApJ*, 270, 20
- Bahcall, N.A. & West, M.J. 1992, *ApJ*, 392, 419
- Bertschinger, E. 1985, *ApJS*, 58, 39
- Borgani, S., Plionis, M., & Kolokotronis, V. 1998, *astro-ph/9812417*
- Croft, R.A.C., & Efstathiou, G. 1994, *MNRAS*, 267, 390

- Dalton, G.B., Croft, R.A.C., Efstathiou, G., Sutherland, W.J., Maddox, S.J., and Davis, M. 1994, MNRAS, 271, 47
- David, L., Forman, W., & Jones, C. 1999, astro-ph/9902129
- De Grandi, S., Bohringer, H., Guzzo, L., Molendi, S., Cinicarini, G., Collins, C., Cruddace, R., Neumann, D., Schindler, S., Schuecker, P., & Voges, W. 1999, ApJ, 514, 148
- Ebeling, H., Voges, W., Böhringer, Edge, A.C., Huchra, J.P., & Briel, U.G. 1996, MNRAS, 281, 799
- Ebeling, H., Edge, A.C., Böhringer, Allen, S.W., Crawford, C.S., Fabian, A.C., Voges, W. & Huchra, J.P. 1998, MNRAS, 301, 881
- Efstathiou, G., Dalton, G.B., Maddox, S.J., & Sutherland, W. 1992, MNRAS, 257, 125
- Eke, V.R, Cole, S., Frenk, C.S., Navarro, J.F. 1996, MNRAS, 281, 703
- Evrard, A.E. & Henry, J.P. 1991, ApJ, 383, 95
- Girardi, M., Giuricin, G., Mardirossian, F., Mezzetti, M., & Boschini, W. 1998, ApJ, 505, 74
- Hamilton, A.J.S. 1993, ApJ, 417, 19
- Kaiser, N. 1986, MNRAS, 222, 323
- Katgert, P., Mazure, A., Perea, J., den Hartog, R., Moles, M., Le Fevre, O., Dubath, P., Focardi, P., Rhee, G., Jones, B., Escalera, E., Biviano, A., Gerbal, D., Giuricin, G. 1996, A & A, 310, 8
- Landy, S.D. & Szalay, A.S. 1993, ApJ, 412, 64
- Ledlow, M.J., Loken, C., Burns, J.O., Owen, F.N., & Voges, W. 1999, ApJ, 516, L53
- Loken, C., Melott, A.L., Miller, C.J. 1999, ApJ Letters in press
- Maddox, S.J., Sutherland, W.J., Efstathiou, G., Loveday, J. 1990a, MNRAS, 243, 692
- Maddox, S.J., Efstathiou, G., Sutherland, W.J. 1990b, MNRAS, 246, 443
- Miller, C., Batuski, D., Slingsland, K., & Hill, J. 1999, ApJ in press
- Moscardini, L., Matarrese, S., De Grandi, S., & Lucchin, F. 1999, astro-ph/9904282
- Navarro, J., Frenk, C., & White, S. 1995, MNRAS, 275, 720
- Nichol, R.C., Briel, U.G., & Henry, J.P. 1994, MNRAS, 267, 771
- Peacock, J.A. & West, M.J. 1992, MNRAS, 259, 494
- Postman, M., Huchra, J. P., & Geller, M. J. 1992, ApJ, 384, 404 (PHG)
- Ratcliffe, A., Shanks, T., Parker, Q. & Fong, R. 1998, MNRAS, 296, 173.
- Slingsland, K.A., Batuski, D.J, Miller, C.M., Haase, S., Michaud, K., & Hill, J.M. 1998, ApJS, 115, 1
- Sutherland, W. 1988, MNRAS, 234, 159
- Szalay, A. & Schramm, D. 1985, Nature, 314, 718
- Vikhlinin, A., McNamara, B.R., Forman, W., Jones, C., Quintana, H., & Hornstrup A. 1998, ApJ, 502, 558
- Voges, W., Ledlow, M.J., Owen, F.N., & Burns J.O. 1999, submitted to AJ
- Willmer, C., Da Costa, L.N., & Pellegrini, P.S. 1998, AJ, 115, 869

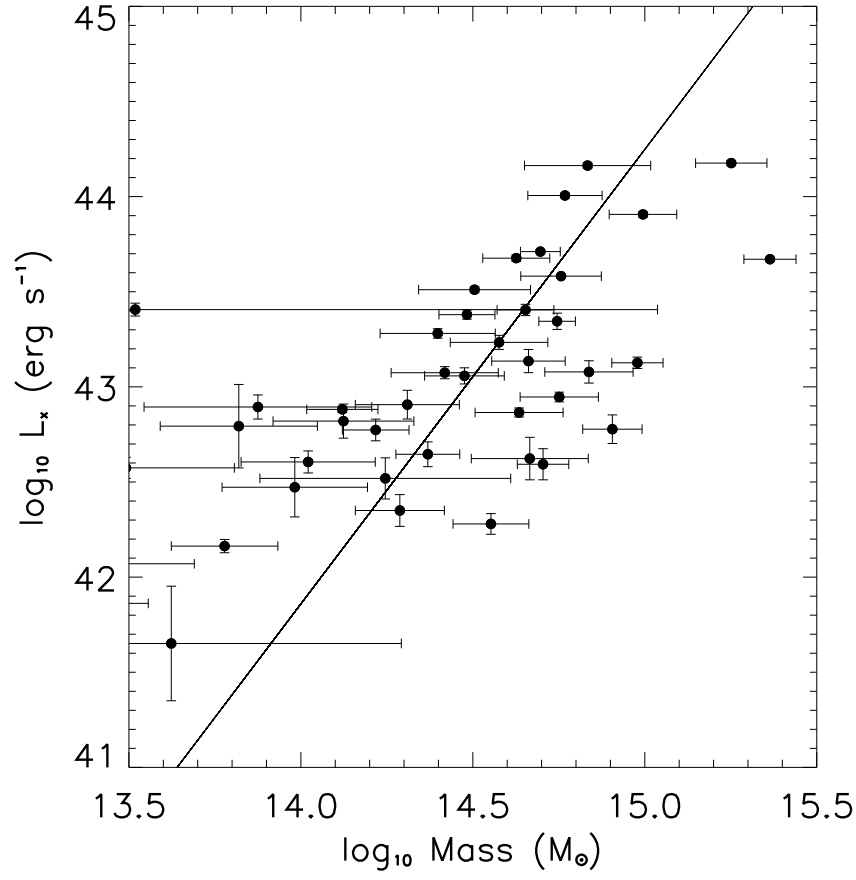


Figure 1. The $L_x - M$ relation for a volume-limited sample ($z \leq 0.09$) of X-ray bright Abell clusters. The cluster virial masses were published by Girardi et al. 1998. The line is an outlier-resistant, error-weighted best fit with a slope of 2.38 ± 1.3 .

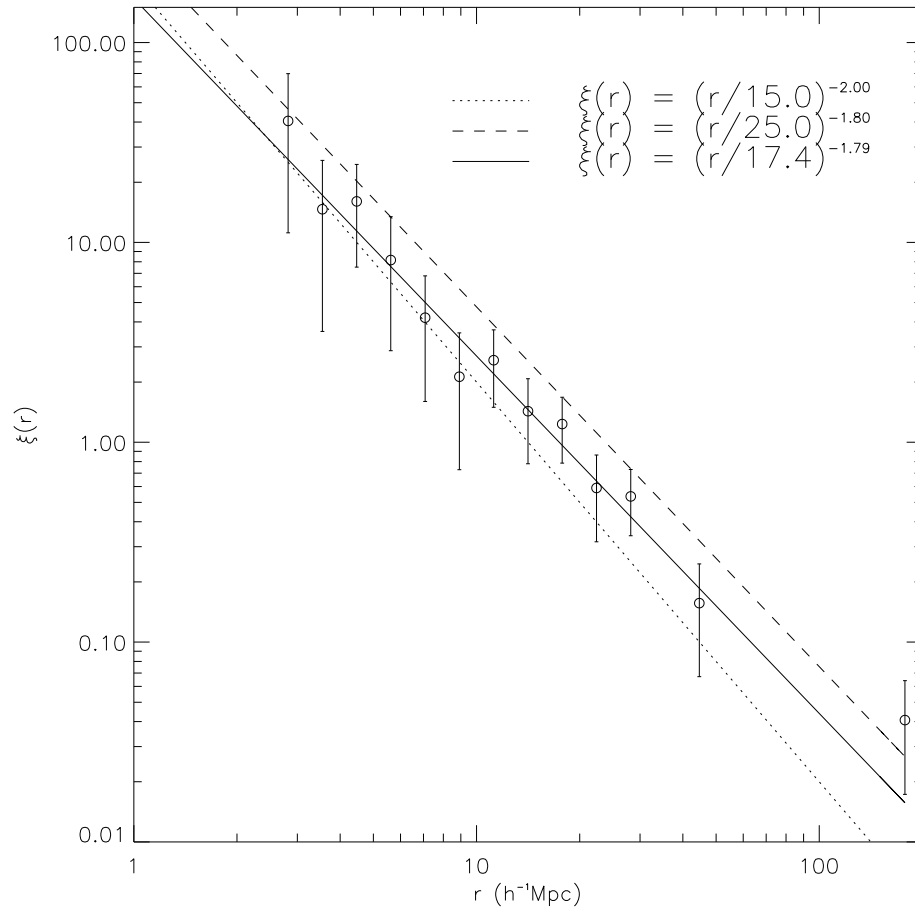


Figure 2. $\xi(r)$ for the Voges et al Sample 1 ($R \geq 0$ Abell clusters). The dashed-line and dotted-line correspond to the two enveloping results for r_0 and γ from Bahcall & Soneira (1983) (dashed) and Efstathiou et al. (1992) (dotted).

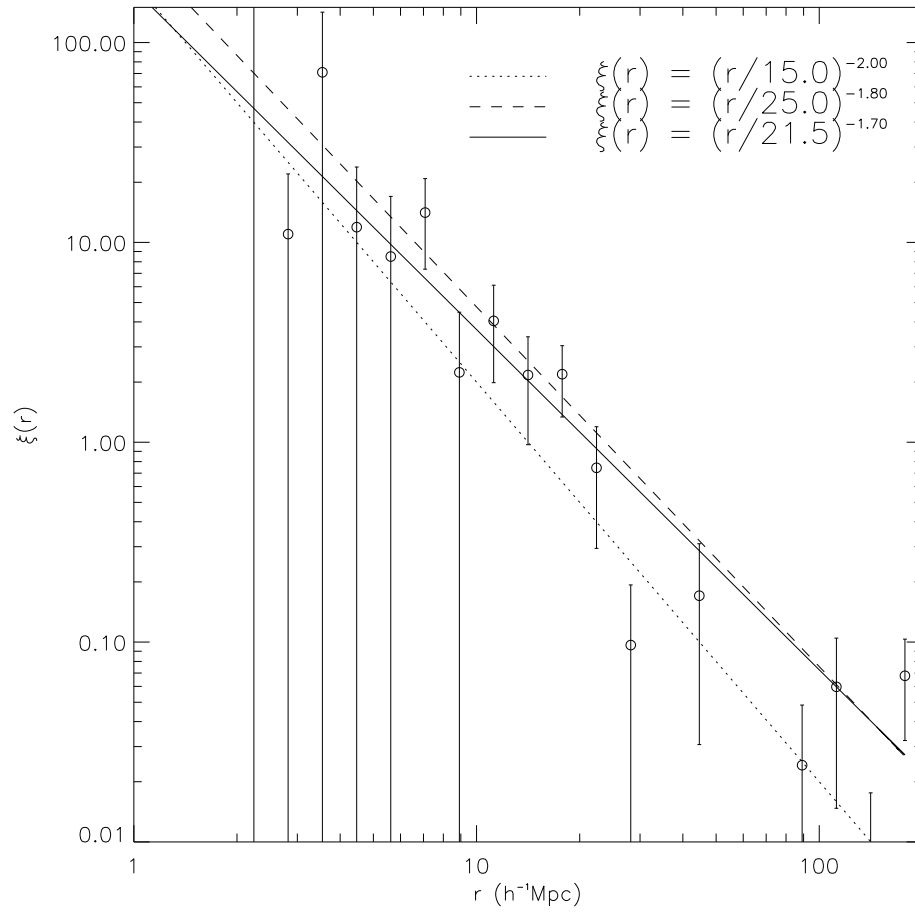


Figure 3. $\xi(r)$ for the Voges et al. Sample 3 ($R \geq 1$ Abell clusters). The dashed-line and dotted-line correspond to the two enveloping results for r_0 and γ from Bahcall & Soneira (1983) (dashed) and Efstathiou et al. (1992) (dotted).

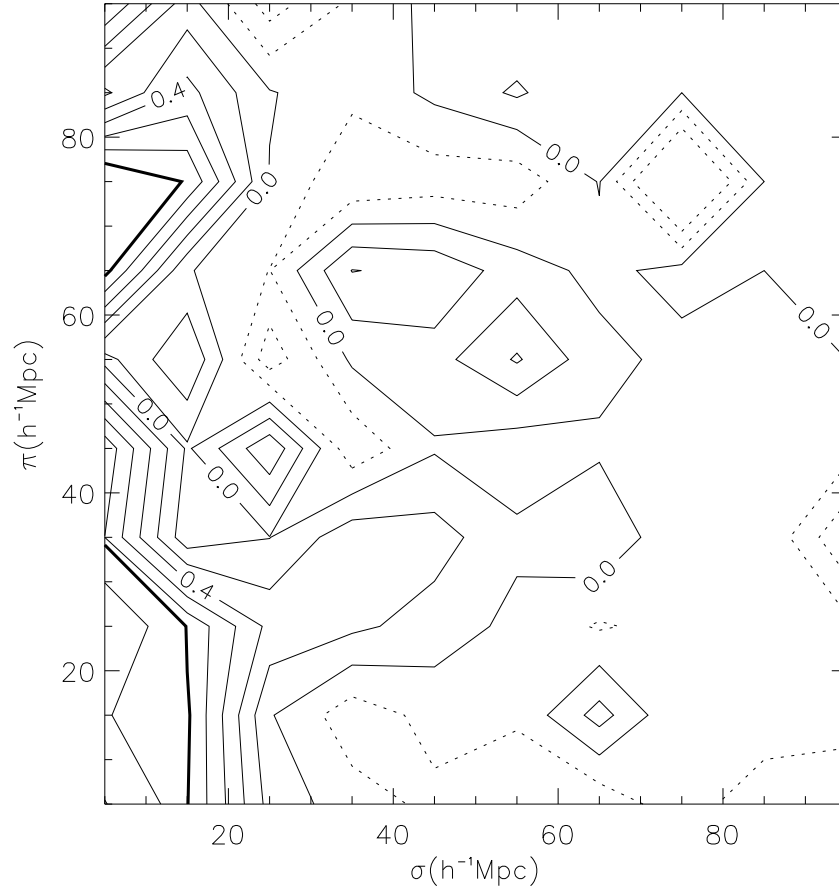


Figure 4. Contour plot of $\xi(\sigma, \pi)$ for the Voges et al. Sample 1 ($R \geq 0$ Abell clusters). The heavy contour corresponds to $\xi(\sigma, \pi) = 1$.

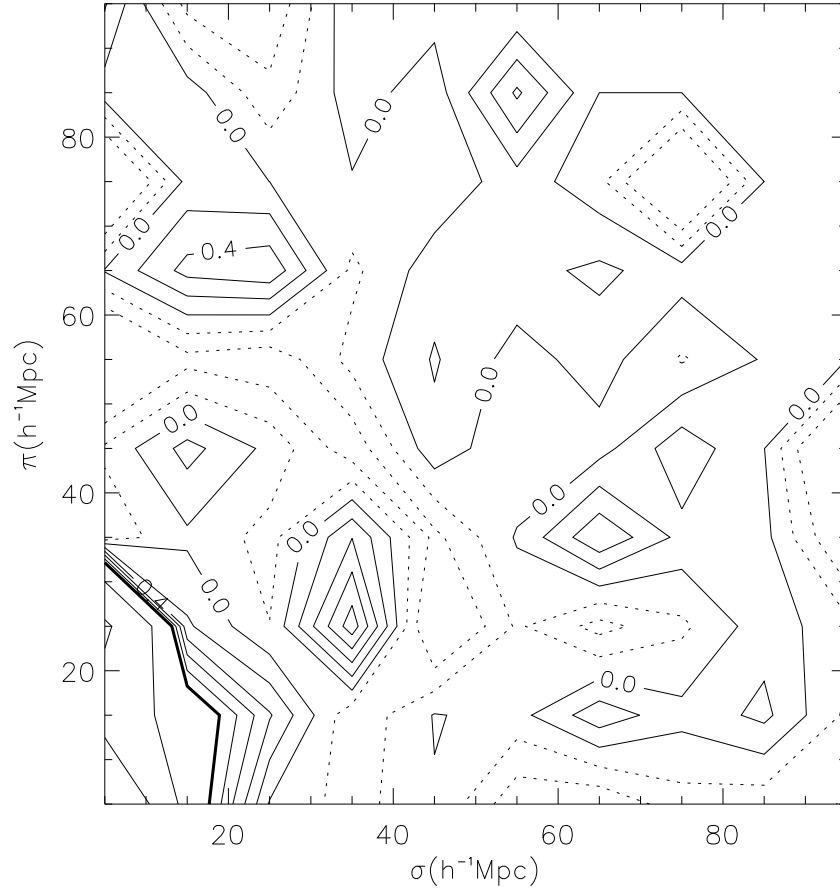


Figure 5. Contour plot of $\xi(\sigma, \pi)$ for the Voges et al. Sample 3 ($R \geq 1$ Abell clusters). The heavy contour corresponds to $\xi(\sigma, \pi) = 1$.

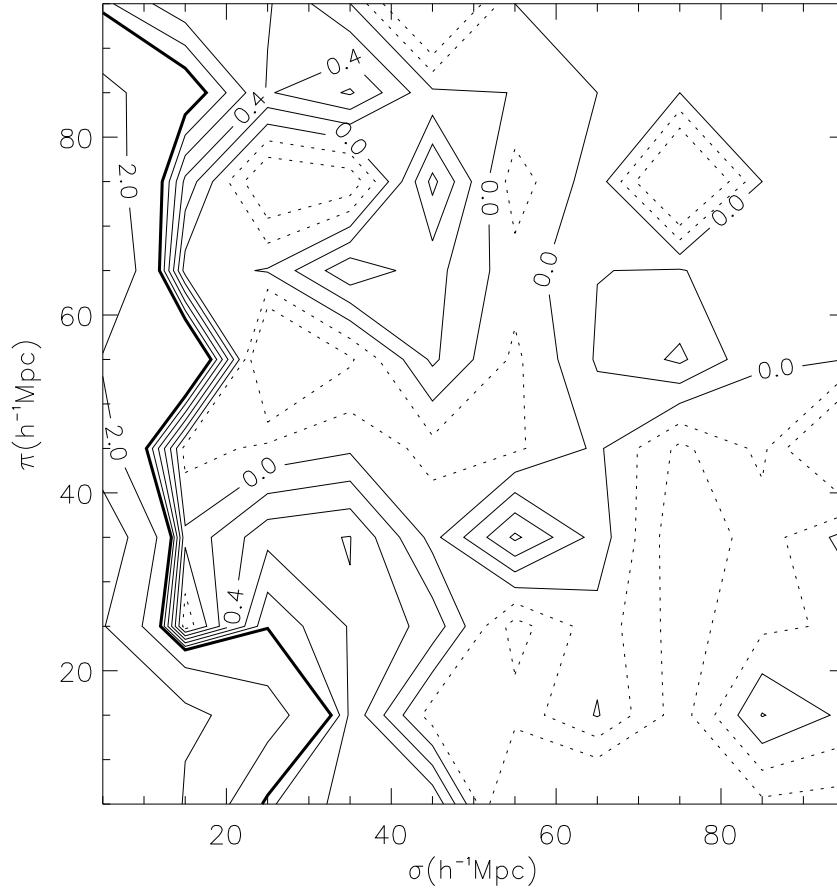


Figure 6. Contour plot of $\xi(\sigma, \pi)$ for the XBACs sample. The heavy contour corresponds to $\xi(\sigma, \pi) = 1$.

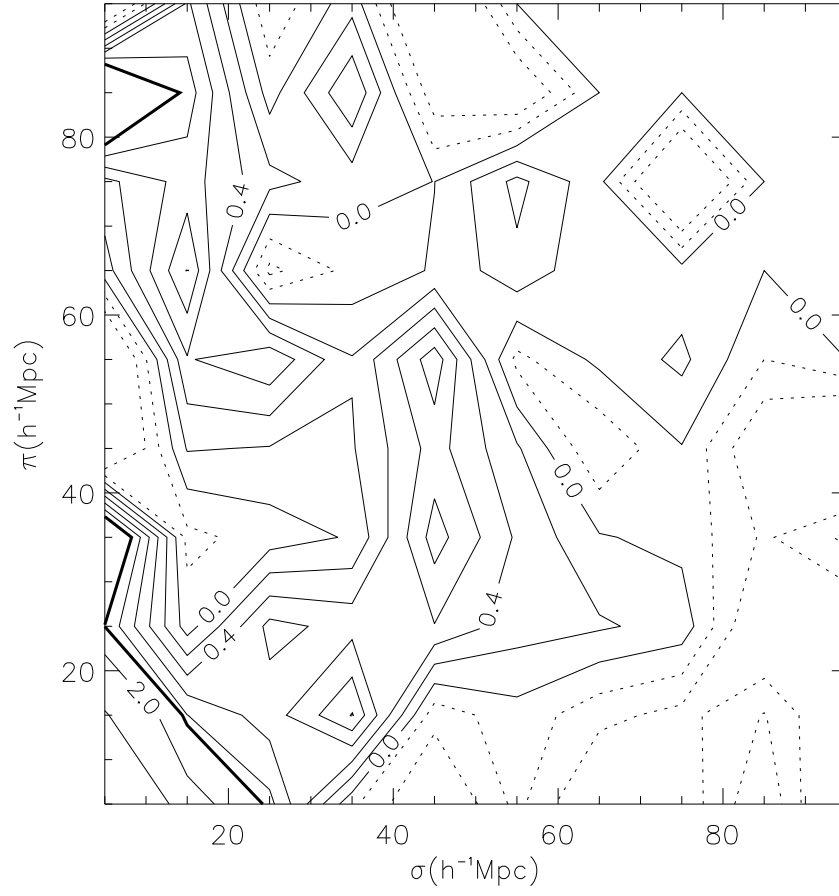


Figure 7. Contour plot of $\xi(\sigma, \pi)$ for the RASS1 clusters. The heavy contour corresponds to $\xi(\sigma, \pi) = 1$.